A cast-in-place fabrication of high performance epoxy composites cured in an in-situ synthesized 3D foam of nanofibers

Nabil Kadhim, Ahsan Zaman, Man Jiang, Ying li, Xue Yang, Jianhui Qiu, Zuowan Zhou

PII: S1359-8368(20)33542-3

DOI: https://doi.org/10.1016/j.compositesb.2020.108495

Reference: JCOMB 108495

To appear in: *Composites Part B*

Received Date: 12 June 2020

Revised Date: 10 September 2020

Accepted Date: 21 October 2020

Please cite this article as: Kadhim N, Zaman A, Jiang M, li Y, Yang X, Qiu J, Zhou Z, A cast-in-place fabrication of high performance epoxy composites cured in an in-situ synthesized 3D foam of nanofibers, *Composites Part B* (2020), doi: https://doi.org/10.1016/j.compositesb.2020.108495.

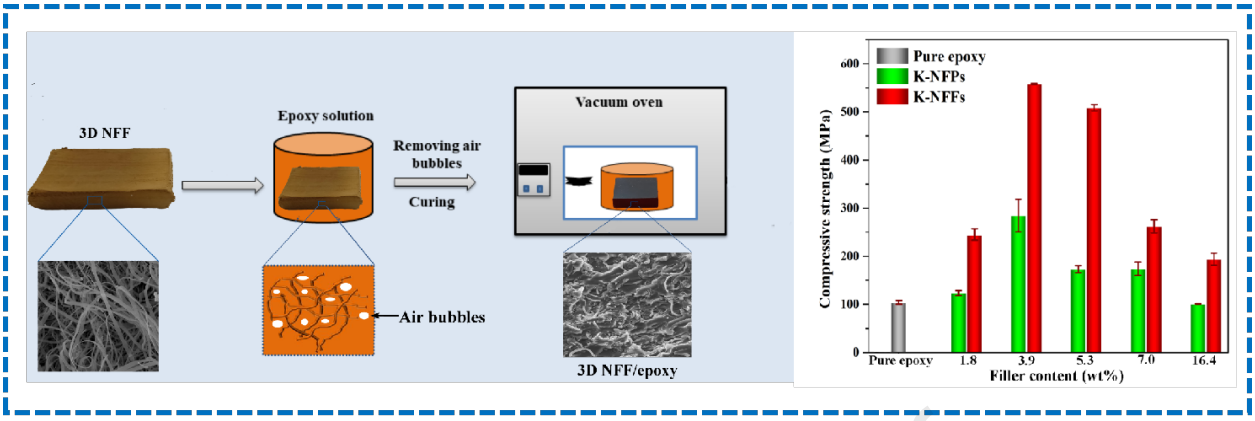

A cast-in-place fabrication of high performance epoxy composites cured in an in-situ synthesized 3D foam of nanofibers

Nabil Kadhim[1, 2], Ahsan Zaman[1], Man Jiang[1, *], Ying li[1], Xue Yang[1], Jianhui Qiu[3], Zuowan Zhou[1, *]

[1] Key Laboratory of Advanced Technologies of Materials (Ministry of Education), School of Materials Science and Engineering, Southwest Jiaotong University, Chengdu 610031, China;

[2] Technical College-Baghdad, Middle Technical University (Ministry of Education), Baghdad 10074, Iraq;

[3] Department of Machine Intelligence and Systems Engineering Faculty of Systems Engineering, Akita Prefectural University, Akita, 015-0055, Japan.

ABSTRACT

A cast-in-place process is usually adopted to prepare bicontinuous composites which display good mechanical properties and excellent comprehensive performance. But the construction of an intercommunicating porous skeleton seems to be cumbersome and low efficient. Here we report a three-dimensional nanofibers foam (3D NFF), which has been fabricated and applied to enhance epoxy resin composite. The 3D NFF skeletons with densities from 0.028 to 0.218 g/cm^3 were fabricated by regulating the conditions for the nanofiber growth. The 3D NFFs were conveniently modified with a silane coupling agent to improve the interface interaction with the epoxy matrix. Compared to the pure epoxy, the compressive strength of the cast-in-place processed 3D NFFs/epoxy composite was improved by 436.8% at loading of 3.9 wt%, and the flexural strength was increased by 133.5% at loading of 5.3 wt%. While the compressive and flexural strength of the

NFPs/epoxy composite prepared through traditional mixing method was increased by 173.6% at loading of 3.9 wt%, and 63.1% at loading of 5.3 wt%, respectively.

*corresponding author.

E-mail address: **jiangman1021@swjtu.edu.cn** (M.Jiang), **zwzhou@swjtu.edu.cn** (Z. Zhou)

Keywords: Three-dimensional nanofibers foam, Cast-in-place process, Epoxy composites, Mechanical properties

1. Introduction

Epoxy resin is an ideal thermosetting polymer for the development of new composites for building and structural materials, owing to their high tensile, compressive, and flexural strengths, and resistance to chemicals, *etc.* While, the cured epoxy resins with a high cross-linking density leads to an adverse brittle property, which causes absorb relatively little energy before fracture and thus weaken their mechanical performance [1]. Nanoparticles are broadly adopted to improve the mechanical strength of epoxy, *e.g.*, carbon nanotubes (CNTs), graphene oxide (GO), metallic oxide and nanoclays, which are commonly introduced into the epoxy resin by solution mixing method [2-8]. The nanoparticles tend to agglomerate in the as-prepared composite for the high aspect ratio and Van der Waals force, which decreases the load transfer efficiency at the interface [9]. Even the homogeneous dispersion of nanoparticles might re-agglomerate during the curing process of epoxy [10]. Lots of research works have been carried out for solving the distribution of nano-carbon fillers in the epoxy resin by chemical functionality, high-speed shear mixing, and applying ultrasound waves [11-13]. However, sometimes, the enhancement effect lost due to the damaged microstructure of the carbon fillers by the modification process or by the high-speed shearing and ultrasound wave. It has been studied that the tensile strength of

MWCNTs/epoxy composites incremented to 17.5% better than that of the neat epoxy with sonication assisted dispersion [12]. Likewise, other studies showed that the epoxy composites containing 0.3 wt% of MWCNTs grafted with amine group exhibited 154% improvement in the flexural strength compared to the neat epoxy [14]. As to our work before, the helical carbon nanotubes were excellent to improve the flexural toughness of epoxy composites compared to the straight MWCNTs, due to the better mechanical intertwining from the helical shape of the carbon nanotubes [15].

Recently, 3D skeleton nanofibers enhanced composite has drawn much attention, for it can reduce the agglomeration of the nanofiller in the polymer matrix, ensuring most of the stress being transferred throughout the 3D filler skeleton [16-19]. Besides, materials with porous structure provide an opportunity for the direct infiltration of low viscous epoxy to fabricate epoxy-based composites, which makes them easily penetrate into the 3D porous structures [20-22]. To improve the interfacial property is crucial for such 3D fibers skeletons enhanced epoxy composites [16, 17, 23-25]. The chemical oxidation [26] and coupling agents treatment [27] have been extensively reported to be efficient to enhance the interfacial property of the nanofiber enhanced polymer composites. It is reasonably expected that the aggregation of the nanoparticles, which usually causes property deterioration[28], can be avoided by using three-dimensional nanofibers foam (3D NFF) to enhance epoxy composites, other than homogenous distribution of nanofibers (NFs) in the epoxy matrix.

In this work, three-dimensional nanofibers foam (3D NFF) with tunable density was prepared by an in-situ growth method. The 3D NFF was applied to fabricate a novel epoxy nanocomposite through a cast-in-place process. A particular emphasis was on the

compressive and flexural strength of the epoxy composites with the density variation of the as-prepared 3D NFFs enhancement. Furthermore, to understand the strengthening and toughening mechanism of the 3D NFFs/epoxy composite prepared with the cast-in-place method, the NFP/epoxy composite prepared through traditional mixing process was taken for the comparison.

2. Experimental

2.1. Materials

Diglycidyl ether of bisphenol F (EPON 862) and curing agent diethyltoluenediamine (DETDA) were provided by Dongguan Qiancheng plasticizing materials Co., Ltd, Guangdong, China. The nanofibers powder with a diameter of 300–490 nm and the length of 10–40 μm were synthesized by a directly in-situ growth method [29]. Concentrated nitric acid (HNO_3, 63 wt%) and glycidoxypropyltrimethoxysilane (KH560) were acquired from Chengdu Kelong Chemicals Factory Co. Ltd, Chengdu, China**.**

2.2. Preparation and modification of nanofibers foam (NFFs)

The 3D nanofibers foam (NFFs) was prepared via a directly in-situ growth process, using in-situ reduced copper nanoparticles from cupric tartrate precursor [30]. By controlling the concentrations of cupric tartrate from 0.015 to 0.066 g inside the ceramic boat before the growth process, we can obtain 3D nanofibers foam (NFFs) with different densities. The cupric tartrate was heated to 260 °C for 15 min in the furnace in an Argon atmosphere to produce metallic copper nanoparticles. Then, acetylene (C_2H_2) was introduced into the furnace to proceed with a directly in-situ growth process at 260 °C for 2 h to form 3D NFFs [30]. After being prepared, the 3D NFF sample was cut into the desired shape for the epoxy composites process. To improve the interface interaction between the

3D NFF and epoxy resin matrix, the pristine 3D NFFs were acidified by being immersed into dilute HNO_3 aqueous solution, and then functionalized with dilute KH560 solution in water and ethanol mixed solvent for 2 h at pH of 4.5.

2.3. Preparation of the 3D nanofibers foam/epoxy composites

The 3D nanofibers foam/epoxy composites were prepared by the cast-in-place process. The content of the 3D NFF in the epoxy matrix was tuned by using the as prepared 3D NFFs with different densities, which are summarized in Table 1. Typical procedure for the composite preparation is that the epoxy resin (100g) and curing agent (26.4g) were firstly mixed under mechanical stirring. Then the mixture of the epoxy resin and curing agent is impregnated into the 3D NFF under vacuum at 70°C, and kept for 24 h. The resulted composite was cured in an oven at 120 °C for 4 h, and 170°C for 4 h in sequence[31], as shown in Fig. 1. The completely cured composites were cut into standard shapes for compressive and flexural properties measurements. The 3D NFFs were crushed into powder (NFPs) to prepare the NFPs/epoxy composite. The certain amount of NFPs was dispersed in the epoxy with a traditional high shear mixing (3500 rpm for 5 min). The NFPs/epoxy composites were prepared using the same loading (Table 1) and curing condition that were adopted for the NFF/epoxy composites. The pore structure of the as prepared 3D NFFs were characterized by mercury intrusion porosimetry (MIP, Quantachrome Instruments，PoreMaster 33，USA) method as reported [32].

Table 1. The characteristics of the as prepared nanofiber foams (NFFs)

Sample	Average pore diameter (mm)	Total pore volume (ml/g)	Specific surface area (m^2/g)	Density (g/cm^3)
1	3.0830	18.8693	24.4820	0.028 ±0.0008

2	0.0707	8.6141	48.7390	0.060 ±0.0040
3	0.5769	9.4209	65.3250	0.080 ±0.0035
4	1.3860	8.4555	24.3959	0.110 ±0.0046
5	0.2714	2.3547	34.6705	0.218 ±0.0065

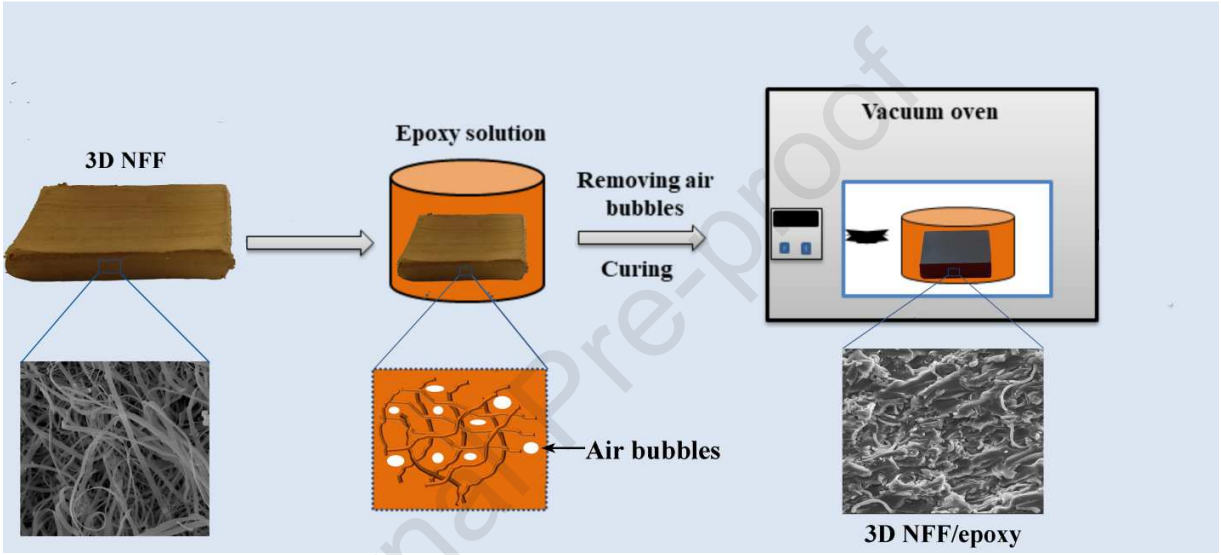

Fig.1 The schematic representation of the cast-in-place process for preparation of the 3D NFFs/epoxy composite.

2.4. Characterization and Testing

Field-emission scanning electron microscopy (FE-SEM, JEOL, JSM-7001F) (Peabody, MA, USA) was applied to study the morphology of 3D NFFs and the fracture surface of 3D NFFs/epoxy composites. The dispersion of the NFFs or NFPs in epoxy was detected with an optical microscope (LEICA, Wetzlar, Germany). The NFPs/Epoxy mixture before curing was dropped on the glass microscope slide for investigation with optical microscope. The NFFs/Epoxy was cut into slide with 0.2 mm in thickness before curing for observation

with optical microscope. The Porosity parameters of 3D nanofibers foam (3D NFFs) were tested by mercury porosimetry (Quantachrome Instruments， PoreMaster 33，USA).

The chemical structure of the pristine NFFs and the silane functionalized nanofibers foam were characterized by Fourier transform infrared spectrometer (FTIR Nicolet 5700, Waltham, MA, USA). X-ray photoelectron spectroscopy (XPS) was utilized to further examining the surface chemical properties of the nanofibers foam, using an Escalab 250Xi spectrometer (Thermo Fisher Scientific, Waltham, MA, USA) with a standard Al K X-ray source (200 W) and the energy of 30 eV.

The surface energy and thermodynamic property of the nanofibers were measured by determining the contact angles that were tested using the shape analysis system, DSA 100 (KRÜSS, Germany) at 23°. The contact angles for each sample were measured five times to calculate the average value.

Compressive and flexural properties were tested on a universal testing machine (PWS-100, China) and (CMT4304, SUST, Sansitaijie, Guangdong, China) at a cross head speed of 2 mm/min, following the standard methods (GB T 1041-2008 and GB1449-2005, respectively). The measurements were conducted at least six times; all the samples were tested at 23°.

3. Results and discussion

3.1. Morphology and structure analysis of the 3D foam skeleton of nanofibers

With a typical synthesis process of the 3D NFFs, the copper (II) tartrate was applied as the catalyst precursor being transferred into the reaction tube, and then the acetylene was inducted into the tube for the catalyzed growth of the 3D skeleton of nanofibers. As shown in Fig. 2, the optical photo of the original 3D skeleton of nanofibers was observed from the Camera lens (Fig. 2a), and the morphology of unmodified and modified 3D NFFs were characterized by a scanning electron microscope (Fig. 2b and 2c). As it can be seen in Fig.

2a, the 3D nanofibers foam with regular and homogeneous shape was obtained by a directly in-situ growth method. The surface structure of the 3D NFFs is primarily clear and porous. After the silane coupling agent modification, the morphology of the 3D nanofibers foam was not changed obviously. The dilute aqueous acid solution and the sequentially silane coupling agent treatment can help maintain the morphology of the nanofibers [5, 6]. The as obtained 3D NFF showed excellent flexibility property for it can be wrapped around the stirring rod, as shown in Fig. 2(a).

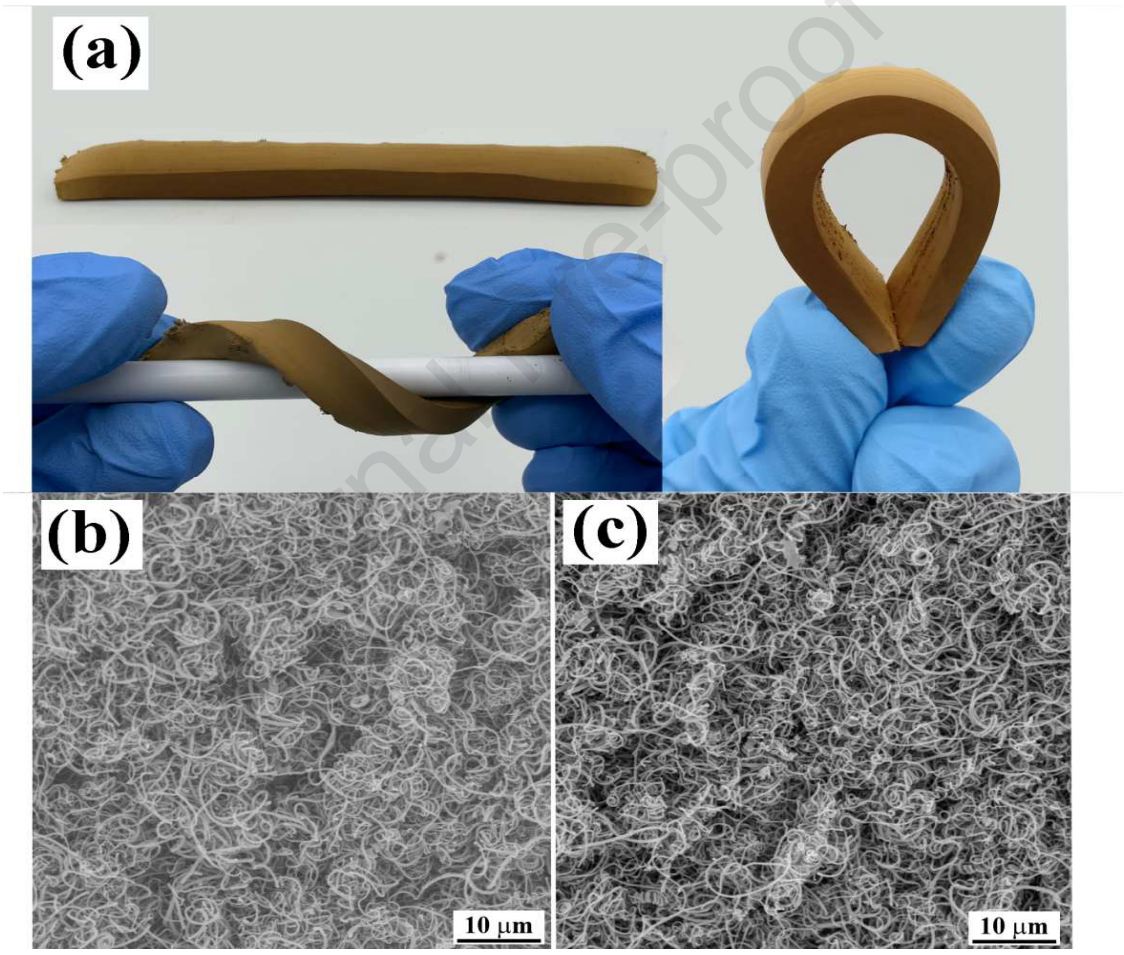

Fig. 2. Optical photos and the morphology of the 3D foam skeleton composed of nanofibers (3D NFFs). (a) The optical photos of the 3D NFFs showing excellent flexibility property, (b) SEM imagines of the as-prepared, and (c) the coupling agent KH560 treated 3D NFFs.

For comparing the chemical structure of the NFFs before and after modification, the FTIR spectra of the as-prepared NFFs, oxidized NFFs and silanized NFFs are displayed in Fig. 3. The peak at 3448 cm^{-1} denotes the stretching vibrations of hydroxyl groups (–OH), which is in agreement with the mechanism of polyacetylene oxidation [30]. The peaks at 2925, 2960, and 1452cm^{-1} are attributed to the C-H vibration in -CH_2. The peak of C=C in the carbon backbone of fiber is seen at 1634 cm^{-1}, and the methane group (C–H) deformation adsorption in the methyl group (CH_3) at 1376 cm^{-1}. As to the oxidized NFFs, the new peak appears at 1718 cm^{-1}, according to the carbonyl group (C=O) stretching vibrations of the (– COOH) [35]. The peaks of the carbonyl group (C-O) show at 1553 cm^{-1}, caused by the alcohol compositions on the carbon nanofibers surface. For the silanized NFFs, the new peaks of Si-C, Si–O–C, and Si–O-Si appear at 1272, 1088, and 803 cm^{-1}, respectively. A C–H peak from the glycidoxypropyltrimethoxysilane molecules was also detected at 870 cm^{-1}. The results approve that the silane molecules are successful covalently bonded to the nanofibers.

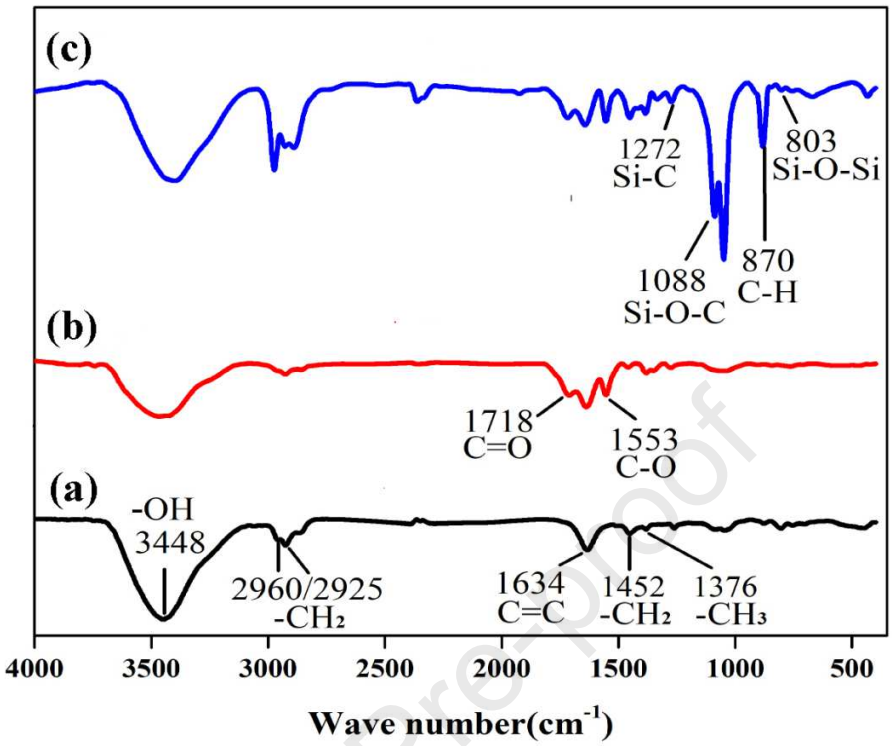

Fig. 3. FTIR spectra of the nanofibers before and after functionalization. (a) Pristine nanofibers (P-NFs), (b) oxidized nanofibers (A-NFs), and (c) silanized nanofibers (K-NFs).

To identify the fundamental compositions on the surface of the NFFs, the XPS spectra are displayed in Fig. 4a. As demonstrated in Fig. 4a, carbon (C1s) and oxygen (O1s) peaks can see in every spectrum. In comparison with the NFFs, the densities of O1s peaks of the functionalized were significantly higher, seemed to indicate that oxygen groups were introduced by the acid oxidation and the silane coupling agent modification. Also, there were two small Si 2s and Si 2p peaks showed in the spectrum of silanized NFFs, which proved that the covalent linkage formed between the KH560 molecules and the surface of the oxidized NFFs. Moreover, to investigate the chemical elements of the pure and modified NFFs, a more detailed analysis of the C1s peak is carried out, and the results were demonstrated in Fig. 4b–e. For the nanofibers foam (NFFs), the C1s peak can be separated

into five fitting curves created from sp3 carbon elements, sp2 carbon elements, in proportion to the C=O, C-H and C–O, respectively. From the spectrum of the acidified nanofibers (NFFs) sample, the two peaks showed at 288.6 and 286.7 eV, which corresponded to O=C–O and C–O–C, respectively. It presented that the carboxyl groups (HO-C=O) were chemically attached to the surface of the oxidized NFFs (Fig. 4c). As shown in the spectrum of silanized NFFs (Fig. 4 d and e), the peaks at 283.3, 103.5, 102.3 and 101.5 eV were attributed to Si–C, Si–O, Si–O–C and Si–O–Si, respectively. It was then reasonably explained the chemical interaction can form between the 3D foam skeleton and the epoxy, due to the coupling agent modification of the 3D NFFs.

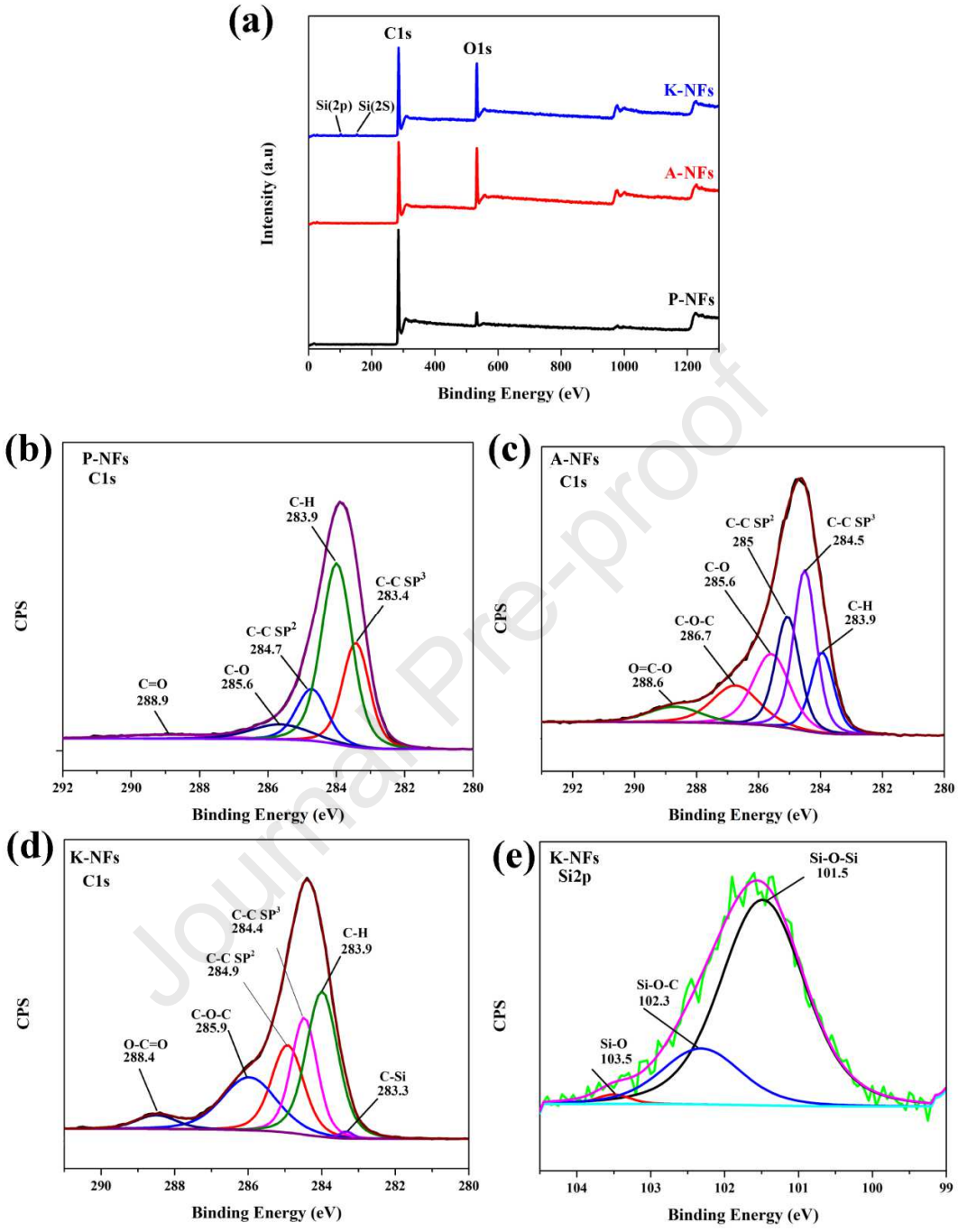

Fig. 4. X-ray photoelectron spectroscopy (XPS) of the nanofibers. (a) XPS survey spectrum of pristine nanofibers (P-NFs), oxidized nanofibers (A-NFs) and silanized nanofibers (K-NFs). High-resolution XPS C1s spectra of (b) P-NFs, (c) A-NFs and (d) K-NFs. (e) High-resolution XPS Si 2p spectra of the K-NFs.

3.2. Surface energy and wettability of the as-prepared nanofibers foam

The contact angle measurement of the nanofibers foams is widely recognized as a crucial parameter to identify the wettability and surface free energy. The NFFs surface free energy is calculated by using the contact angles for three liquids, e.g., deionized water, ethylene glycol, and epoxy resin. The contact angles of these three kinds of liquids on the 3D foam surface were directly measured with the drop form at the point of contact with the surface.

The relationship between the surface energy and the contact angle is express by Young's formula, which shows the state for equilibrium at the solid-liquid interface as given in Eq. (1). In assuming the surface energy of material is composed of a dispersion part and a polar part, it is determined by Eq. (2) [37, 38].

$$\gamma_L(1 + cos\theta) = 2\sqrt{\gamma_S^d \cdot \gamma_L^d} + 2\sqrt{\gamma_S^p \cdot \gamma_L^p} \quad (1)$$

$$\gamma_S = \gamma_S^d + \gamma_S^p \quad (2)$$

where γ_L is the surface tension of liquid; θ is the contact angle between the two kinds of liquid-air interaction, γ_S is a surface free energy of solid, d and p means dispersion and polar component, respectively. The wetting liquids used were epoxy resin (γ_L^d: 41.20 mN/m, γ_L^p: 5.0 mN/m, γ_L: 46.20 mN/m), ethylene glycol (γ_L^d: 31.0 mN/m, γ_L^p: 16.70 mN/m, γ_L: 47.70 mN/m). Contact angles were applied to calculate the surface energies [38, 39]. The surface energy and the contact angle of the 3D NFFs were tested to analyze the interface properties between epoxy and the 3D NFFs, as summarized in Table 2.

It is seen that with KH560 modification, the surface energy of NFFs rise from 42.48 to 44.47 mN/m, and the increment arises from the growth in the polar functional groups

covalently bonded with nanofibers (from 7.20 to 10.84 mJ/m^2) that occurred through the oxidation of surface NFFs.

Table 2. Contact angle and surface energy analysis of 3D nano fibers foam

Samples	contact angle (°)			Surface energy (mJ/m^2)			
	Water	Ethylene glycol	Epoxy	γ_S	γ_S^d	γ_S^p	γ_{12}
Pristine NFFs	146.0±5	32.0±4	29.7±4	42.48	35.28	7.20	0.82
Silanized NFFs	47.8±2	22.9±3	21.0±5	44.47	33.87	10.84	2.63

As seen from the results included in Table 2, after modification with silane coupling agent, the epoxy contact angle decrease from 29.7±4° to 21.0±5°, which was not obvious compared with water and ethylene glycol. However, the surface energy of the 3D NFFs increased considerably from 0.82 to 2.63 mJ/m^2 after the modification, which presented more active sites of unsaturated valence bonds were produced to improve the interface properties of the modified 3D NFF and epoxy.

It was predicted that the surface free energy had played a key role in enhancing the interface interaction between the epoxy resin and the silanized NFFs, which is in accordance with the reports [38, 40]. The silane coupling agent efficiently increased the surface energy of the 3D NFF due to the enhancement of polar groups, which was in accordance with the FTIR (Fig. 3) and XPS (Fig. 4) results. According to the existence of the Si–O, Si–O–C and Si–O–Si functional group on the NFF surface, chemical interaction could form between the nanofibers and the epoxy matrix [35, 36, 38]. Thus the improvement is a consideration of newly created active groups on the surface of the silanized NFFs, which include oxides and silanes elements, as proved by the FTIR spectra and XPS examines (Fig. 3 and 4). Based on the surface energy analysis, the

interfacial tension between the solid and liquid can be calculated through the harmonic-mean equation and geometric-mean equation, as shown in Eq. (3).

The harmonic-mean equation:

$$\gamma_{12} = \gamma_1 + \gamma_2 - 4\left[\frac{\gamma_1^d \gamma_2^d}{\gamma_1^d + \gamma_2^d} + \frac{\gamma_1^p \gamma_2^p}{\gamma_1^p + \gamma_2^p}\right] \quad (3)$$

where $\gamma_{12}$is the interfacial tension of the epoxy with fibers. Superscripts (d and p) refer to the London dispersive and specific components, respectively. The calculated interfacial tension of nanofibers before and after functionalization are shown in Table 2.

It was observed that the interfacial tension of the silanized NFFs demonstrated a high-value of adhesion strengths better than the original NFFs. The results of interfacial energy were consistent with the morphological analysis by SEM images (Fig. S3, Supplementary Information).

In the following work, both the nanofiber particles (NFPs) and the 3D nanofibers foam (NFFs) were surface functionalized to comparably study the effect of cast-in-place and direct mixing processes on the performance of the epoxy nanocomposite.

3.3. Comparisons of the cast-in-place with direct mixing processed composites

The mechanisms for strengthening and toughening of the 3D NFFs/epoxy composites prepared by the cast-in-place method were compared with the traditional filling process for better understanding the mechanical performance of the composites. We compared the mechanical properties of the composites by varying the fibre percentage (0.0, 1.8, 3.9, 5.3, 7.0 and 16.4% in weight) of the NFP or 3D NFFs. As shown in Fig. 5, the 3D NFFs reinforced composites showed higher compressive properties compared to the NFPs/composites. In comparison with the pure epoxy, the compressive strength and strain of the epoxy composite with fiber loading 3.9 wt% prepared by the traditional mixing

process were increased from 104.0 MPa and 61.6% to 284.5 MPa and 80.9%, respectively. While the 3D NFFs prepared by the cast-in-place process, the corresponding values were increased to 558.3 MPa and 115.4% with the same fiber loadings (3.9 wt%), showing in Fig. 5b. The cast-in-place process uses to eliminate concerns about the formation of agglomeration of nanofibers, which usually acts as stress concentrators and potential failure sites in the epoxy. Besides, the modified 3D nanofibers have a network in vertical and horizontal directions in 3D nanofibers foams this form can provide strength on all sides and provides pathways for stress transfer. Furthermore, the addition of flexible 3D nanofibers to the epoxy resin increased the flexibility of the composite. At higher content of scattered fibers over than 3.9 wt% caused decreasing compressive strength and strain compare with the same filling content prepared by the cast-in-place process, the aggregation can lead to forming the stress concentration sites in the epoxy composite. As nanoparticles agglomerate, the interfacial bonding would be lower, and then lead to the poor stress transfer between epoxy and nanofibers.

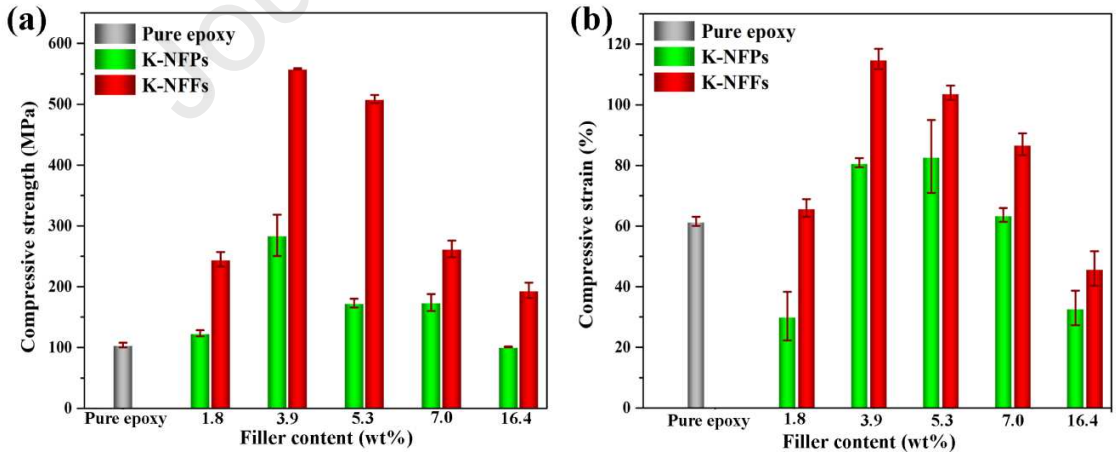

Fig. 5. The compressive properties of the 3D foam skeleton of the nanofibers (3D NFFs)/epoxy composites via cast-in-place method, compared with the nanofibers

(NFPs)/epoxy composites by direct mixing method. (a) Compressive strength, (b) compressive strain.

The flexural properties of pure epoxy and its composite are shown in Fig. 6. It can be seen that the flexural properties of the 3D NFFs enhanced composites were improved higher than that of the NFPs/epoxy composites. The flexural strength of NFP filled composites had the highest value of 143.4 MPa with 3.9 wt% of filler content. With increasing the NFPs loading to 5.3 wt%, the flexural strength of the nanocomposite decreased to 133.4 MPa. A high percentage of scattering fibers could act as defects within the epoxy matrix. While the flexural strength and strain of composites epoxy reinforced by 5.3 wt%, 3D NFFs had a maximum value 228.9 MPa and 7.2%, respectively. In comparison to the composites prepared by the traditional filling process with the same loading (5.3 wt%), the flexural strength and the strain of 3D NFFs are increased by 71.6% and 44%, respectively. Besides, with increased 3D NFFs loading to 7.0 wt%, the flexural strain of functionalized 3D NFFs composites was also increased by 47.1% as compared to the pure epoxy, which is due to the rise in the aspect ratio of the 3D nanofibers in the epoxy composite. While the flexural strain of epoxy composite prepared by the traditional mixing process was improved by 14.3% with the same loading (7.0 wt%). Application of the 3D NFFs to enhance the epoxy composite by the cast-in-place process resolved the agglomeration problem in the preparation of the nanocomposites. The 3D NFFs skeleton considerably decreased the variance in stress locations of 3D NFFs/epoxy composites and highlighted the mechanical efficiency. To disclose the effect of the surface modification on the composite, we also conducted the mechanical characteristics and fracture morphology

289 the pristine 3D NFFs enhanced epoxy composite (Fig. S1 and S2, Supplementary
290 Information).

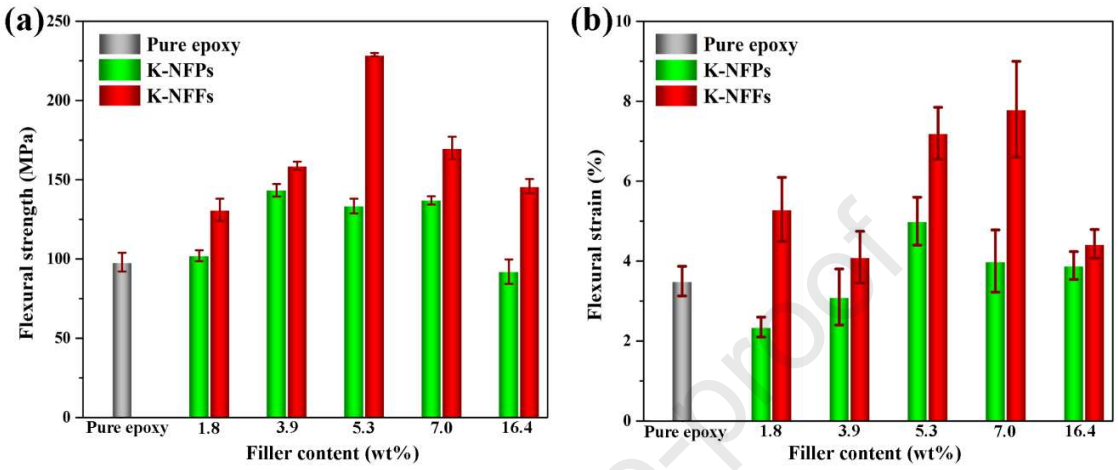

291 **Fig. 6**. The flexural properties of the 3D foam skeleton of the nanofibers (3D NFFs)/epoxy
292 composites prepared via cast-in-place method, compared with the nanofibers (NFPs)/epoxy
293 composites prepared by direct mixing method. Flexural strength (a) and flexural strain (b).

294 3.4. *The comparable analysis of strengthen mechanisms between the cast-in-place and*
295 *traditional mixing processes*

296 The surface and the fracture morphology of the 3D NFF/epoxy composite prepared by
297 cast-in-place process and the NFPs/epoxy composite prepared via traditional mixing
298 process were as shown in Fig. 7. The surface morphology of the composites before curing
299 is as can be seen in Fi. 7 a and b. Owing to the open porous of the 3D NFFs , the epoxy can
300 be easily infiltrated [41]. Whereas agglomeration and sedimentation of nanofiber particles
301 (NFPs) are obvious (Fig. 7b) in the NFPs/epoxy composite, which results from Coulomb
302 attractions and Van der Waals forces [42-44]. Likewise, the dispersion state and interfacial
303 affinity were confirmed from the fracture surface morphology of 3D NFF/epoxy and
304 NFP/epoxy composites, as shown in Fig. 7 a1 and b1.

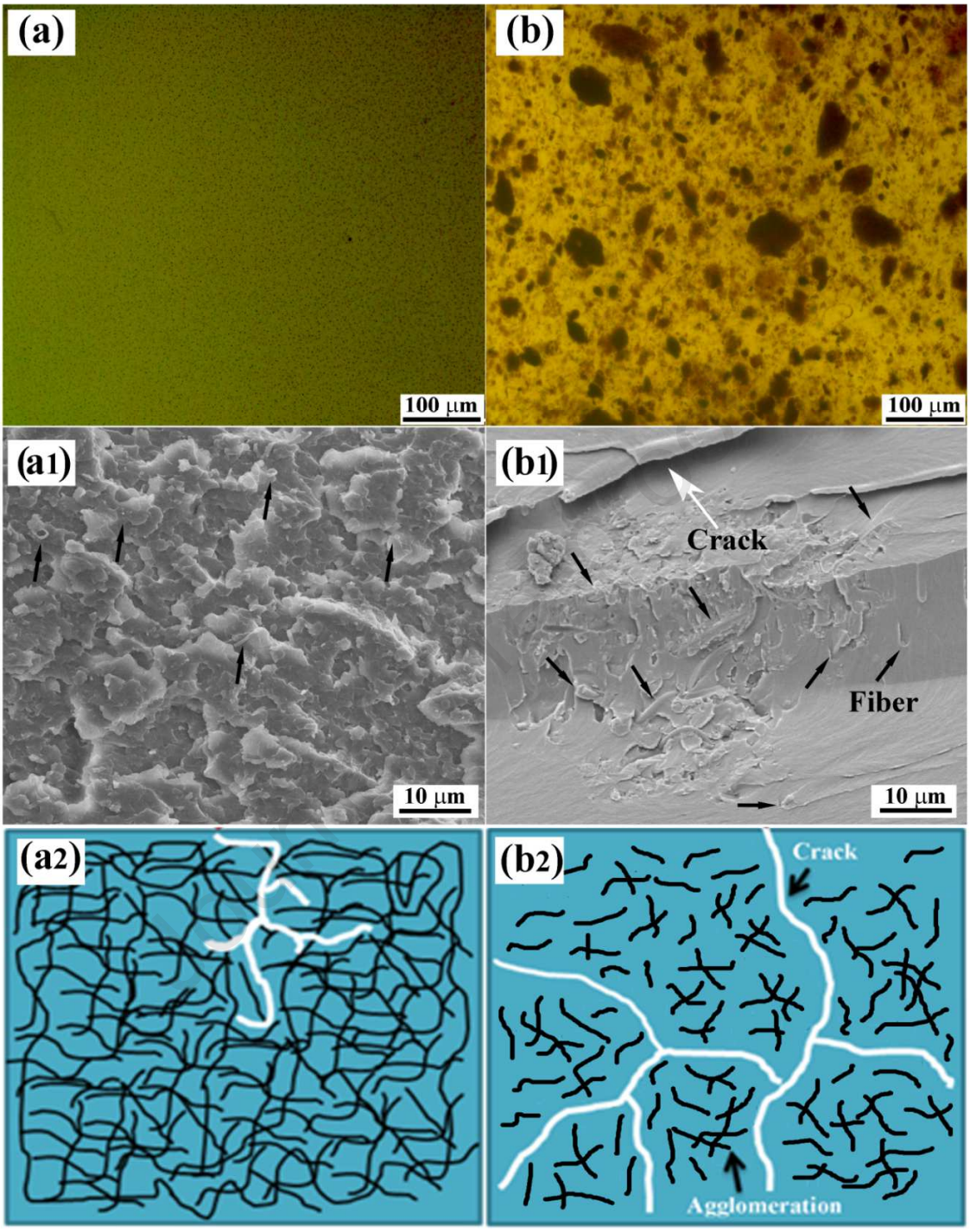

Fig. 7. Comparison of the composites samples prepared with cast-in-place and traditional mixing processes. The optical microscope surface of 3D NFFs/epoxy composite prepared by the cast-in-place process (a), and NFPs/epoxy composite prepared by

traditional mixing process (b); the SEM images of the fracture surfaces of 3D NFFs/epoxy composite prepared by cast-in-place process (a1), and the NFPs/epoxy composite prepared by traditional mixing process (b1); (a2) and (b2) are the illustration of the development of the cracks in the 3D NFFs/epoxy and NFPs/epoxy composites, respectively. The contents of the nano filler in the composites are 3.9 wt%.

The fracture surface of the 3D NFFs/epoxy composite (Fig. 7 a1) was of homogeneous micro-cracks, ascribing to the stress transfer through the 3D NFFs. The crack deflection and coalescence of micro-cracks resulted in a rough surface. Also, a porous interconnected skeleton and its capability to bend and flex in response to the stress allowed effective energy dissipation [45]. As shown in Fig. 7 b1, the fracture surface of the NFPs/epoxy composite presents the typical brittle fracture with extensive micro-cracks distribution and relatively smooth. The 3D NFFs takes important role in improving the fracture strength of 3D NFFs/epoxy composites. On one hand, the fracture energy is dissipated when the cracks reaches the 3D NFF skeleton. On the other, the stable and well-dispersed nano fibers caused the crack deflection, which enhanced the fracture strength of the composite. Furthermore, as shown in the spectrum of silanized NFFs (Fig. 4 d and e), the silane coupling agent was connected to the nano fibers through covalent bonds. It was then reasonably explained the chemical bonding formed between the 3D foam skeleton and the epoxy.

As expected, inside the 3D NFFs strengthened epoxy composite processed with the cast-in-place method, the nano fibers involves crack-bridging, the bridging process can suppress crack propagation, as illustrated in Fig. 7 a2. The crack energy profligates by forming good dispersion and interfacial adhesion between the nanofibers and the matrix

(Fig. S3, Supplementary Information). Therefore, the maximum fracture toughness has been obtained by the cast-in-place process using 3D NFFs in the matrix with improved interface adhesion. The agglomeration of nanofibers in the polymer matrix can cause cracks formation and propagate quickly, resulting in decreasing of the strength of composites accordingly, as illustrated in Fig. 7 b2 [46].

4. Conclusion

This work demonstrated a new strategy for the preparation of 3D nanofibers foam (NFFs) with tunable densities towards a high-performance bicontinuous composite by the cast-in-place process. Compared with the scattered nanofibers within the epoxy matrix prepared via direct mixing process, the 3D NFFs skeletons with cast-in-place method has overcome the issue of agglomeration of nanofiller in the epoxy matrix. This process has also reduced the consumption of organic solvents to disperse the nanofiller during the traditional direct mixing process. As compared to the pure epoxy, the compressive strength of the NFFs/epoxy composite prepared by the cast-in-place method was improved by 436.8%, while the NFPs/epoxy composite prepared by the traditional filling process was increased by 173.5% with the same loadings (3.9 wt%). Besides, the flexural strength of the NFFs/epoxy was improved by 133.5%, while the NFPs/epoxy composite prepared via the traditional filling process was improved by 63.1% with the same loading (5.3 wt%). This work has explored an effective strategy for developing high-performance nanocomposites, which could be an excellent candidate for automobile and aircraft industry.

Acknowledgement:

This work was facially supported by the National Natural Science Foundation of China (No. 51573149) and the Sichuan Province Science and Technology Program (No.

2018GZ030 and No. 2019ZDZX0018). We also thank the Analytical and testing centre of Southwest Jiaotong University for the SEM test.

Appendix A. Supplementary material

References

[1] Yeping Wu, Zhongyun Gu, Maobin Chen, Chunhua Zhu, and Hong Liao, "Effect of functionalization of multi-walled carbon nanotube on mechanical and viscoelastic properties of polysulfide-modified epoxy nanocomposites," *High Performance Polymers,* vol. 291, pp. 51–160, 2017.

[2] X.-J. Shen, X.-Q. Pei, Y. Liu, and S.-Y. Fu, "Tribological performance of carbon nanotube–graphene oxide hybrid/epoxy composites," *Composites Part B: Engineering,* vol. 57, pp. 120-125, 2014.

[3] M.-T. Le and S.-C. Huang, "Thermal and Mechanical Behavior of Hybrid Polymer Nanocomposite Reinforced with Graphene Nanoplatelets," *Materials,* vol. 8, pp. 5526-5536, 2015.

[4] S.-Y. Yang, W.-N. Lin, Y.-L. Huang, H.-W. Tien, J.-Y. Wang, C.-C. M. Ma*, et al.*, "Synergetic effects of graphene platelets and carbon nanotubes on the mechanical and thermal properties of epoxy composites," *Carbon,* vol. 49, pp. 793-803, 2011.

[5] S. Chatterjee, F. Nafezarefi, N. H. Tai, L. Schlagenhauf, F. A. Nüesch, and B. T. T. Chu, "Size and synergy effects of nanofiller hybrids including graphene nanoplatelets and carbon nanotubes in mechanical properties of epoxy composites," *Carbon,* vol. 50, pp. 5380-5386, 2012.

[6] Fabiana de C. Fim, Nara R. S. Basso, Ana P. Graebin, Denise S. Azambuja, and G. B. Galland, "Thermal, Electrical, and Mechanical Properties of Polyethylene–Graphene Nanocomposites Obtained by In situ Polymerization," *J. APPL. POLYM. SCI,* vol. 128, pp. 2630–2637, 2013.

[7] R. Metz, L. Diaz, R. Aznar, L. Alvarez, V. Flaud, S. Ananthakumar*, et al.*, "Carbon Nanotubes-Epoxy Composites: The role of acid treatment in Thermal and Electrical Conductivity," *Experimental Heat Transfer,* 2016.

[8] Q. Zhang, G. Wu, F. Xie, N. Li, Y. Huang, and L. Liu, "Mechanical properties of carbon fiber composites modified with nano-SiO2in the interphase," *Journal of Adhesion Science and Technology,* vol. 28, pp. 2154-2166, 2014.

[9] R. Atif, I. Shyha, and F. Inam, "The degradation of mechanical properties due to stress concentration caused by retained acetone in epoxy nanocomposites," *RSC Adv.,* vol. 6, pp. 34188-34197, 2016.

[10] P.-C. Ma, S.-Y. Mo, B.-Z. Tang, and J.-K. Kim, "Dispersion, interfacial interaction and re-agglomeration of functionalized carbon nanotubes in epoxy composites," *Carbon,* vol. 48, pp. 1824-1834, 2010.

[11] E. Pullicino, W. Zou, M. Gresil, and C. Soutis, "The Effect of Shear Mixing Speed and Time on the Mechanical Properties of GNP/Epoxy Composites," *Applied Composite Materials,* vol. 24, pp. 301-311, 2016.

[12] A. Montazeri and M. Chitsazzadeh, "Effect of sonication parameters on the mechanical properties of multi-walled carbon nanotube/epoxy composites," *Materials & Design (1980-2015),* vol. 56, pp. 500-508, 2014.

[13] L. Pan, J. Ban, S. Lu, G. Chen, J. Yang, Q. Luo*, et al.*, "Improving thermal and mechanical properties of epoxy composites by using functionalized graphene," *RSC Adv.,* vol. 5, pp. 60596-60607, 2015.

[14] P. Garg, B. P. Singh, G. Kumar, T. Gupta, I. Pandey, R. K. Seth*, et al.*, "Effect of dispersion conditions on the mechanical properties of multi-walled carbon nanotubes based epoxy resin composites," *Journal of Polymer Research,* vol. 18, pp. 1397-1407, 2010.

[15] N. Kadhim, Y. Mei, Y. Wang, Y. Li, F. Meng, M. Jiang*, et al.*, "Remarkable Improvement in the Mechanical Properties of Epoxy Composites Achieved by a Small Amount of Modified Helical Carbon Nanotubes," *Polymers (Basel),* vol. 10, Oct 5 2018.

[16] S. Chandrasekaran, W. V. Liebig, M. Mecklenburg, B. Fiedler, D. Smazna, R. Adelung*, et al.*, "Fracture, failure and compression behaviour of a 3D interconnected carbon aerogel (Aerographite) epoxy composite," *Composites Science and Technology,* vol. 122, pp. 50-58, 2016.

[17] C. D. Garcia, K. Shahapurkar, M. Doddamani, G. C. M. Kumar, and P. Prabhakar, "Effect of arctic environment on flexural behavior of fly ash cenosphere reinforced epoxy syntactic foams," *Composites Part B: Engineering,* vol. 151, pp. 265-273, 2018.

[18] K. Wang, W. Wang, H. Wang, L. Liu, Z. Xu, H. Fu*, et al.*, "3D graphene foams/epoxy composites with double-sided binder polyaniline interlayers for maintaining excellent electrical conductivities and mechanical properties," *Composites Part A: Applied Science and Manufacturing,* vol. 110, pp. 246-257, 2018.

[19] L. Jin, L. Liu, J. Fu, C. Fan, M. zhang, M. Li*, et al.*, "3D interconnected nanosheets architecture as transition layer and nanocontainer for interfacial enhancement of carbon fiber/epoxy composites," *Industrial & Engineering Chemistry Research,* 2019.

[20] J. Li, L. Wei, W. Leng, J. F. Hunt, and Z. Cai, "Fabrication and characterization of cellulose nanofibrils/epoxy nanocomposite foam," *Journal of Materials Science,* vol. 53, pp. 4949-4960, 2018.

[21] J. H. Hodgkin, G. P. Simon, and R. J. Varley, "Thermoplastic toughening of epoxy resins: A critical review," *Polymers for Advanced Technologies,* vol. 9, pp. 3-10, 2015.

[22] J. A. King, D. R. Klimek, I. Miskioglu, and G. M. Odegard, "Mechanical properties of graphene nanoplatelet/epoxy composites," *Journal of Applied Polymer Science,* vol. 128, pp. 4217-4223, 2013.

[23] K. Wang, W. Wei, H. Wang, L. Liu, Z. Xu, H. Fu*, et al.*, "3D graphene foams/epoxy composites with double-sided binder polyaniline interlayers for maintaining excellent electrical conductivities and mechanical properties," *Composites Part A Applied Science & Manufacturing,* p. S1359835X18301805, 2018.

[24] A. Zaman, F. Huang, M. Jiang, W. Wei, N. Kadhim, and Z. Zhou, "Fabrication of Enhanced Epoxy Composite by Embedded Hierarchical Porous Lignocellulosic Foam," *Renewable Energy,* 2019.

[25] W. W. Ying Li, Ying Wang, Nabil Kadhim, Yuan Mei, Zuowan Zhou, "Construction of highly aligned graphene-based aerogels and their

epoxy composites towards high thermal conductivity," *Journal of Materials Chemistry C,* vol. 7, 2019.

[26] J. Ding, Y. Huang, T. Han, and Y. Wang, "Synthesis of functionalized graphene oxide nanoflakes using silane coupling agents," *High Performance Polymers,* vol. 28, pp. 147-155, 2015.

[27] S. Yu, K. H. Oh, J. Y. Hwang, and S. H. Hong, "The effect of amino-silane coupling agents having different molecular structures on the mechanical properties of basalt fiber-reinforced polyamide 6,6 composites," *Composites Part B: Engineering,* vol. 163, pp. 511-521, 2019.

[28] T. Glaskova, M. Zarrelli, A. Borisova, K. Timchenko, A. Aniskevich, and M. Giordano, "Method of quantitative analysis of filler dispersion in composite systems with spherical inclusions," *Composites Science & Technology,* vol. 71, pp. 1543-1549, 2011.

[29] J. Xian, J. Man, Z. Zuowan, Z. Qun, L. Jun, W. Dingchuan*, et al.*, "Gas-induced formation of Cu nanoparticle as catalyst for high-purity straight and helical carbon nanofibers," *Acs Nano,* vol. 6, p. 8611, 2012.

[30] X. Jian, M. Jiang, Z. Zhou, M. Yang, J. Lu, S. Hu*, et al.*, "Preparation of high purity helical carbon nanofibers by the catalytic decomposition of acetylene and their growth mechanism," *Carbon,* vol. 48, pp. 4535-4541, 2010.

[31] Y. Zhou, F. Pervin, L. Lewis, and S. Jeelani, "Fabrication and characterization of carbon/epoxy composites mixed with multi-walled carbon nanotubes," *Materials Science and Engineering: A,* vol. 475, pp. 157-165, 2008.

[32] P. Valášek, R. D'Amato, M. Müller, and A. Ruggiero, "Mechanical properties and abrasive wear of white/brown coir epoxy composites," *Composites Part B: Engineering,* vol. 146, pp. 88-97, 2018.

[33] J. Kathi and K. Y. Rhee, "Surface modification of multi-walled carbon nanotubes using 3-aminopropyltriethoxysilane," *Journal of Materials Science,* vol. 43, pp. 33-37, 2007.

[34] Y. Wang, Y. Mei, Q. Wang, W. Wei, F. Huang, Y. Li*, et al.*, "Improved fracture toughness and ductility of PLA composites by incorporating a small amount of surface-modified helical carbon nanotubes," *Composites Part B: Engineering,* vol. 162, pp. 54-61, 2019.

[35] H. Khosravi and R. Eslami-Farsani, "On the mechanical characterizations of unidirectional basalt fiber/epoxy laminated composites with 3-glycidoxypropyltrimethoxysilane functionalized multi-walled carbon nanotubes–enhanced matrix," *Journal of Reinforced Plastics and Composites,* vol. 35, pp. 421-434, 2015.

[36] T. Lu, M. Jiang, Z. Jiang, D. Hui, Z. Wang, and Z. Zhou, "Effect of surface modification of bamboo cellulose fibers on mechanical properties of cellulose/epoxy composites," *Composites Part B: Engineering,* vol. 51, pp. 28-34, 2013.

[37] D. Liu, W. Li, N. Zhang, T. Huang, J. Yang, and Y. Wang, "Graphite oxide-driven miscibility in PVDF/PMMA blends: Assessment through dynamic rheology method," *European Polymer Journal,* vol. 96, pp. 232-247, 2017.

[38] W.-K. Choi, H.-I. Kim, S.-J. Kang, Y. S. Lee, J. H. Han, and B.-J. Kim, "Mechanical interfacial adhesion of carbon fibers-reinforced polarized-polypropylene matrix composites: effects of silane coupling agents," *Carbon letters,* vol. 17, pp. 79-84, 2016.

[39] C. J, "Handbook of Adhesives and Sealants: General Knowledge, Application Techniques, New Curing Techniques (ed.P.Cognard)," *Elsevier Science,* 2006.

[40] K. Song, J. Lee, S.-O. Choi, and J. Kim, "Interaction of surface energy components between solid and liquid on wettability, and its application to textile anti-wetting finish," *Polymers,* vol. 11, p. 498, 2019.

[41] Y. Ni, L. Chen, K. Teng, J. Shi, X. Qian, Z. Xu*, et al.*, "Superior Mechanical Properties of Epoxy Composites Reinforced by 3D Interconnected Graphene Skeleton," *Acs Applied Materials & Interfaces,* vol. 7, pp. -, 2015.

[42] P. C. Ma, S.-Y. Mo, B.-Z. Tang, and J.-K. Kim, "Dispersion, interfacial interaction and re-agglomeration of functionalized carbon nanotubes in epoxy composites," *Carbon,* vol. 48, pp. 1824-1834.

[43] Q. Zhang, J. Wu, L. Gao, T. Liu, W. Zhong, G. Sui*, et al.*, "Dispersion stability of functionalized MWCNT in the epoxy–amine system and its effects on mechanical and interfacial properties of carbon fiber composites," *Materials & Design,* vol. 94, pp. 392-402, 2016.

[44] P.-C. Ma, N. A. Siddiqui, G. Marom, and J.-K. Kim, "Dispersion and functionalization of carbon nanotubes for polymer-based nanocomposites: A review," *Composites Part A: Applied Science and Manufacturing,* vol. 41, pp. 1345-1367, 2010.

[45] T. P. Yong, Y. Qian, C. Chan, T. Suh, and A. Stein, "Epoxy Toughening with Low Graphene Loading," *Advanced Functional Materials,* vol. 25, 2014.

[46] L. C. Tang, Y.-J. Wan, D. Yan, Y.-B. Pei, L. Zhao, Y.-B. Li*, et al.*, "The effect of graphene dispersion on the mechanical properties of graphene/epoxy composites," *Carbon,* vol. 60, pp. 16-27.

Highlights

1. The 3D nanofibers foam has been prepared and adopted to fabricate high-performance epoxy composite by a cast-in-place process.
2. The compressive strength of the as prepared 3D NFFs/epoxy composite was improved by 436.8% than the pure epoxy resin.
3. The flexural strength of the as prepared 3D NFFs/epoxy composite was also 133.5% higher than the pure epoxy resin.

Dear editor,

We have submitted the manuscript named "*High-performance epoxy composites fabricated with 3D nanofibers foam：Preparation, Properties and Toughening mechanism" (JCOMB-D-20-00432R1)* to **Composites Part B: Engineering** at June 9th, 2020. According to the reviewers` valuable comments, we have made the point-to-point responses and revised the whole paper carefully. The name of the manuscript is changed into *"A cast-in-place fabrication of high performance epoxy composites cured in an in-situ synthesized 3D foam of nanofibers"* as respond to the reviewer`s suggestion. We prepared the 3D nanofibers foam samples, and then the NFFs/epoxy composites again to test their tensile strength, which has been included in the "Response to the Reviewers" as well as added in the "supplementary material".

We sincerely appreciate the editor and the reviewers` helpful questions and suggestions for our work. We hope the revised manuscript can meet the requirement of **Composites Part B: Engineering**.

Sincerely yours,

Man Jiang

Declaration of interests

☑ The authors declare that they have no known competing financial interests or personal relationships that could have appeared to influence the work reported in this paper.

☐The authors declare the following financial interests/personal relationships which may be considered as potential competing interests: